

RESEARCH

Open Access



Target of Rapamycin is a crucial regulator of photosynthesis and nutrient metabolism partitioning in *Nannochloropsis gaditana*

Zhengying Zhang^{1,2,3}, Yanyan Li^{1,2,3}, Shu Yang^{1,2,3}, Shuting Wen^{1,2,3}, Hongmei Zhu² and Hantao Zhou^{1,2,3*}

Abstract

Utilizing microalgae as “photosynthetic cell factories” for compound production holds significant potential for sustainable carbon neutrality. However, the inherent inefficiency of algal photosynthesis, a limiting factor for productivity, represents a critical area for enhancement. Among the key regulatory mechanisms, the Target of Rapamycin (TOR), essential for cell growth regulation and known for its conserved structure across eukaryotes, remains underexplored in *Nannochloropsis gaditana*. In this study, we identified conserved component of the TOR complex in *N. gaditana*. Rapamycin (RAP) effectively inhibited photosynthetic growth and enhanced lipid accumulation in *N. gaditana*, as demonstrated by sensitivity tests. Transcriptomic analysis revealed that NgTOR modulates multiple intracellular metabolic and signaling pathways. Specifically, genes associated with photosynthesis and chlorophyll synthesis were significantly down-regulated following NgTOR inhibition. Additionally, genes involved in carbon metabolism, the TCA cycle, and amino acid biosynthesis were markedly reduced, while those related to lipid metabolism were up-regulated, resulting in stunted cell growth and increased lipid accumulation. Furthermore, blocking photosynthesis with DCMU significantly reduced the transcriptional activity of TOR-related complexes, highlighting a bidirectional regulatory interaction. These findings underscore the pivotal role of the TOR signaling pathway in regulating photosynthesis, carbon metabolism, and lipid metabolism in *N. gaditana*, setting the stage for further studies on photosynthetic autotrophy and lipid metabolic pathways in this species.

Keywords TOR, RAP, Photosynthesis, DCMU, Lipid metabolic

Introduction

Microalgae are abundant sources of fats, polysaccharides, proteins, carotenoids, and other bioactive substances with unique functionalities [1]. They hold promise as

potential substitutes for agricultural products in both food and feed applications, and they can serve as biofactories for drug production [2]. However, the growth of microalgae is constrained by various factors, including lighting conditions, energy conversion efficiency, and the efficiency of carbon dioxide fixation [3]. Light is crucial in regulating the growth and development of photosynthetic organisms [4, 5]. Comprehending the mechanisms behind microalgae growth is critically important due to its vast scientific and practical implications, especially in optimizing biomass yield [6]. Improving microalgae’s photosynthetic efficiency, thereby enhancing light-to-biomass conversion, presents a viable strategy to address the constraints on biomass yield [7, 8]. Growth regulation

*Correspondence:

Hantao Zhou

htzhou@xmu.edu.cn

¹ State Key Laboratory of Marine Environmental Science, Xiamen University, Xiamen 361000, China

² College of Ocean and Earth Sciences, Xiamen University, Xiamen 361000, China

³ State-Province Joint Engineering Laboratory of Marine Bioproducts and Technology, Xiamen University, Xiamen 361000, China



© The Author(s) 2025. **Open Access** This article is licensed under a Creative Commons Attribution-NonCommercial-NoDerivatives 4.0 International License, which permits any non-commercial use, sharing, distribution and reproduction in any medium or format, as long as you give appropriate credit to the original author(s) and the source, provide a link to the Creative Commons licence, and indicate if you modified the licensed material. You do not have permission under this licence to share adapted material derived from this article or parts of it. The images or other third party material in this article are included in the article’s Creative Commons licence, unless indicated otherwise in a credit line to the material. If material is not included in the article’s Creative Commons licence and your intended use is not permitted by statutory regulation or exceeds the permitted use, you will need to obtain permission directly from the copyright holder. To view a copy of this licence, visit <http://creativecommons.org/licenses/by-nc-nd/4.0/>.

via photosynthetic gene expression is closely associated with the TOR signaling pathway [9, 10].

The TOR protein is highly conserved among eukaryotes, with a molecular size of approximately 280 kDa, and it plays a crucial role in regulating cell growth while sensing nutritional and energy statuses in eukaryotic organisms [11]. Initially identified in budding yeast during the screening of RAP-resistant mutants, TOR is a serine/threonine protein kinase belonging to the Phosphatidylinositol 3-kinase-related kinase family [12, 13]. It comprises five conserved domains, namely HEAT repeats, FAT (adhesion target), FRB (FKBP12, FK506 drug binding protein 12/RAP binding), kinase, and FATC domains. HEAT repeats directly bind to the promoter and 5' UTR region of 45S rRNA through its leucine zipper domain, thereby regulating 45S rRNA synthesis [14, 15]. The TORC1 complex primarily consists of TOR proteins, LST8, and Raptor6 (regulatory-associated protein of TOR), which regulate translational, trophic, and energetic signaling and are sensitive to RAP. In contrast, the TORC2 complex comprises TOR, Rictor (the rapamycin-insensitive partner of TOR, LST8, and SIN1, and is not sensitive to rapamycin. Notably, the TORC2 complex has not yet been identified in plants or other photosynthetic organisms [16].

TOR kinases are critical for integrating nutrient and energy inputs to regulate cell growth in lower eukaryotes [11]. They promote cell growth by facilitating anabolic processes, such as translation, ribosome biogenesis, and transcription, while suppressing catabolic processes, including autophagy and mRNA degradation [17, 18].

In yeast and mammals, TOR functions through two complexes, TORC1 and TORC2, which have been extensively studied, revealing diverse functions of TOR signaling in plants [12]. In plants, only one TORC complex has been identified, primarily localized to the inner membrane and nucleus, where it functions in response to varying environmental conditions [19, 20]. Studies in plants have shown that regulating TOR signaling pathway genes can enhance photosynthetic efficiency and increase biomass yield. In *Arabidopsis thaliana*, overexpression of TOR genes reduces chlorophyll degradation under stress conditions, improving stress tolerance [21]. Conversely, inducible knockdown of TOR-related genes in *A. thaliana* causes growth arrest due to reduced polysaccharide accumulation, ultimately resulting in decreased plant biomass, organ size, and cell size [20].

Recent TOR-related studies in algae have revealed that algae, like plants, possess TOR proteins, but lack the TORC2 core components Rictor/AVO3 and Sin1/AVO1 [22]. Current research on the TOR signaling pathway has primarily focused on the model microalga *C. reinhardtii*, where a large TORC1 complex has been identified [23,

24]. Early genetic analyses in *C. reinhardtii* confirmed the presence of TOR, RAPTOR, and Lst8 genes, which are essential for its survival, highlighting the evolutionary conservation of the TOR pathway [23]. Moreover, RAP treatment has been shown to inhibit *C. reinhardtii* cell growth [25, 26]. In *C. reinhardtii*, an FKBP12-deficient mutant, named rap2, exhibits resistance to RAP. Studies have shown that the interaction between LST8 and TOR is essential for maintaining TOR activity, ensuring the structural integrity and functionality of the TOR complex [27, 28]. Notably, conditional depletion or chemical inhibition of TOR in *C. reinhardtii* induces global metabolic reprogramming, resulting in the transient accumulation of energy reserves such as starch and triacylglycerols (TAGs) [29]. This shift underscores TOR's role as a metabolic gatekeeper, redirecting carbon and energy flow toward storage compounds when growth ceases, a process directly relevant to biofuel production strategies.

Beyond its role in growth regulation, TOR signaling and its subunits have been implicated in photosynthetic function in algae. As the primary source of fixed carbon and energy, photosynthesis is tightly regulated, with the TOR pathway integrating internal and external signals to adjust photosynthetic capacity. Under nutrient-sufficient conditions, TOR activity supports a high rate of protein synthesis, promoting the assembly and turnover of photosynthetic complexes, as well as the expression of genes involved in light harvesting and electron transport. Conversely, TOR inhibition reduces photosynthetic efficiency and decreases photosynthetic protein levels, reflecting a cellular strategy to conserve energy during resource scarcity. While the precise mechanisms linking TOR to photosynthetic regulation remain unclear, it is likely that the phosphorylation and turnover of photosynthetic proteins are indirectly influenced by TOR complex stabilization. In the red alga *Cyanidioschyzon merolae*, TOR signaling regulates starch synthesis by modulating the phosphorylation state of CmGLG1, a glycogenin required for starch/glycogen initiation [30]. Additionally, proteomic analyses in *C. reinhardtii* suggest that TOR regulates the expression of chloroplast-targeted proteins, potentially influencing chloroplast structure and function [13, 25].

N. gaditana is a marine unicellular alga with a long history of use in aquaculture and eicosapentaenoic acid (EPA) production, highlighting its significant economic and industrial value [31]. Its small, easily manipulated genome makes it an ideal model for metabolic engineering [32, 33]. Additionally, the TOR signaling pathway plays a central role in regulating growth and lipid metabolism in microalgae, making it a key focus for research on the precise control of algal growth and metabolic processes [15, 34, 35]. This study investigated the TOR signaling pathway and its role in regulating photosynthetic

growth and lipid partitioning in *N. gaditana*. A conserved NgTOR protein complex-related gene was identified in *N. gaditana*, highlighting its evolutionary conservation. Drug sensitivity tests using RAP were conducted to examine the effects of TOR inhibition on photosynthesis, growth, and lipid accumulation. Additionally, histological analysis provided preliminary insights into the central regulatory role of the TOR signaling pathway in photosynthesis, carbon metabolism, and lipid metabolism in *N. gaditana*.

Result

Component of TOR complex is conserved in *Nannochloropsis gaditana*

TOR kinases are pivotal in regulating a variety of essential cellular processes as the catalytic subunits of two distinct protein complexes, TORC1 and TORC2 [11]. While TORC1's structure and function are universally conserved among eukaryotes, including algae and plants, TORC2's core protein is conspicuously absent in photosynthetic organisms [4, 23]. In *N. gaditana*, only a single conserved TOR protein (NgTOR) was identified, exhibiting a maximum similarity of 50.5% to the PtTOR protein (Supplementary Table S1). Essential TORC1 components, RAPTOR and LST8, were detected in *N. gaditana* (Fig. 1A), while TORC2's crucial proteins, RICTOR and SIN1, were absent.

The TORC1 complex primarily comprises the proteins TOR, RAPTOR, and LST8, with corresponding genes also named *TOR*, *RAPTOR*, and *LST8* (Fig. 1A). NgTOR features N-terminal HEAT repeats, FAT, FRB, catalytic, and FATC domains. LST8 possesses a WD40 tandem repeat sequence, facilitating its interaction with the TOR kinase domain to enhance selective binding to downstream substrates for regulatory purposes. RAPTOR is characterized by an N-terminal RNC structural domain, HEAT repeats, and WD40 tandem repeats, contributing significantly to the stability, catalytic functionality, and substrate affinity of the TORC1 complex (Fig. 1B). Sequence comparisons indicate that NgTOR's catalytic domain is highly conserved, exhibiting the greatest similarity across species (Fig. 1C).

The phylogenetic tree illustrates the evolutionary relationships of TOR proteins across different species, with high bootstrap values supporting the reliability of the analysis. Both AtTOR and CrTOR clustered together, highlighting the evolutionary similarity of TOR proteins between higher plants and green algae. NgTOR formed a distinct branch alongside ScTOR, suggesting that the TOR proteins of *N. gaditana* may possess unique functional characteristics. Additionally, diatom TORs (PtTOR and TpTOR) clustered closely, demonstrating high conservation, while CmTOR (from red algae) appeared on

the most distant branch, indicating a significant evolutionary divergence. These findings indicate that TOR is highly conserved across eukaryotes, yet species-specific differences exist, particularly in algae, where the diversity of TOR may play a crucial role in adapting to varying ecological environments (Fig. 1D). The evolutionary relationships among FKBP12 proteins from different species were also analyzed. The results revealed that species such as NsFKBP12, StFKBP12, and OsFKBP12 clustered together, indicating a closer evolutionary relationship. In contrast, NgFKBP12 and AtFKBP12 formed a separate branch, reflecting distinct evolutionary patterns. Additionally, ScFKBP12 and CrFKBP12 were positioned on a more distant branch, suggesting a significant evolutionary divergence from other species. These clustering patterns imply that FKBP12 proteins retain conserved functions across species, while the divergence observed in certain branches may correspond to species-specific functional adaptations (Fig. 1E).

Nannochloropsis gaditana is highly sensitive to RAP

The growth inhibition of *N. gaditana* was studied using RAP during the logarithmic growth phase of *N. gaditana* cultures. This study aimed to establish the correlation between *N. gaditana* growth and varying concentrations of RAP inhibitor, and to analyze the resulting growth rate of *N. gaditana* based on experimental data. Subsequently, the dynamic changes in *N. gaditana* growth induced by RAP inhibition were examined and interpreted.

The concentration gradient of RAP ranged from 0 to 50 nM and was cultured under light conditions. The optimal concentration of RAP for *N. gaditana* was determined to be 10 nM by monitoring the growth changes of *N. gaditana* (Fig. 2A). Following RAP treatment, algal cell growth was not completely halted according to flow cytometry, but a severe reduction in cell growth was observed (Fig. 2B). Moreover, RAP treatment significantly affected cell size, resulting in a decrease in algal cell size (Fig. 2C). Additionally, chlorophyll fluorescence analysis indicated a substantial decrease after RAP treatment (Fig. 2D). The algal cell population was notably distinct from the wild type (Supplementary Figure S1), suggesting an impact on chlorophyll synthesis. This illustrates that the inhibition of TOR activity influences chlorophyll synthesis in *N. gaditana* and consequently its photosynthesis, leading to growth arrest of algal cells. Importantly, this growth arrest is reversible and non-lethal.

Effect of TOR on photosynthesis of *Nannochloropsis gaditana*

Algal cells treated with 10 nM RAP were collected via centrifugation, and photosynthetic parameters were subsequently measured to investigate the regulatory

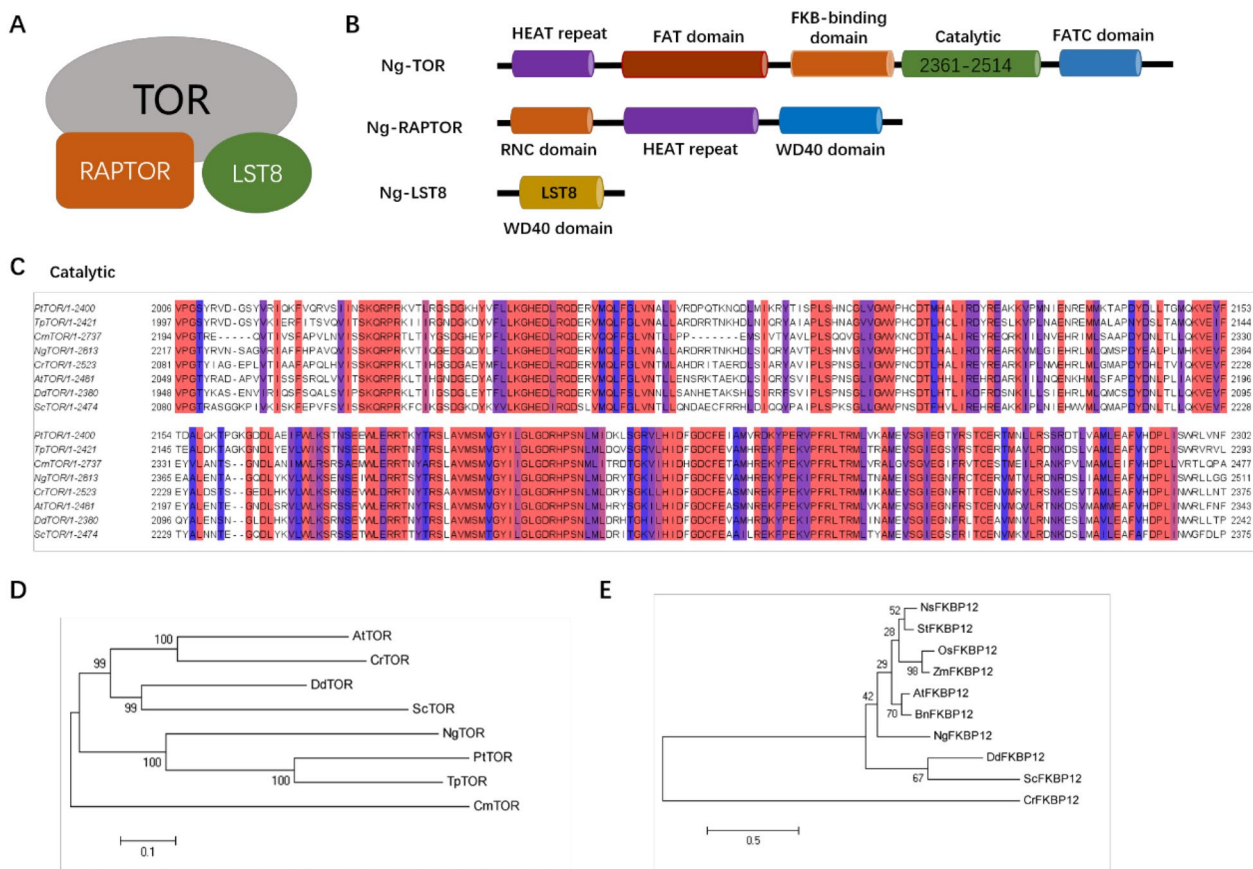


Fig. 1 Analysis of the Structure and Sequence of NgTOR. **A** Modeling the TOR Protein Complex. Represented by gray, orange, and green, respectively. **B** Analysis of conserved structural domains of three complex proteins, NgTOR, NgRAPTOR and NgLst8. **C** Sequence alignment of the catalytic domains of NgTOR protein and homologs from other species. Red indicates conserved sequences, while blue denotes sequences with over 70% identity. **D** Phylogenetic analysis of TOR from *N. gaditana* and related species. Constructed using the Neighbor-Joining method via MEGA5 software, the phylogenetic trees display bootstrap percentages based on 1000 replicates. Other species mainly include *Phaeodactylum tricornutum* (Pt), *C. reinhardtii* (Cr), *C. merolae* (Cm), *Thalassiosira pseudonana* (Tp), *A. thaliana* (At), *Dictyostelium discoideum* (Dd), and *Saccharomyces cerevisiae* (Sc). **E** Phylogenetic analysis of FKBP12 from *N. gaditana* and related species. Constructed using the Neighbor-Joining method via MEGA5 software, the phylogenetic trees display bootstrap percentages based on 1000 replicates. Other species mainly include *C. reinhardtii* (Cr), *C. merolae* (Cm), *A. thaliana* (At), *D. discoideum* (Dd), *S. cerevisiae* (Sc), *Oryza sativa* (Os), *Solanum tuberosum* (St), *Zea mays* (Zm), *Nicotiana sylvestris* (Ns), and *Brassica napus* (Bn)

potential of the TOR signaling pathway on algal photosynthesis. Measurements were conducted using a 440-nm measurement light, focusing on the chloroplast Photosystem II (PSII) light-trapping antenna's light energy conversion, including the maximum photochemical efficiency (Fv/Fm), actual photosynthetic quantum yield (Y(II)), and relative electron transfer rate (rETR).

The results revealed a significant impact on photosynthesis following RAP treatment, primarily evident in a notable decrease in Fv/Fm and Y(II) of *N. gaditana* from 24 to 96 h post-treatment (Fig. 3A). Specifically, Fv/Fm values in the treatment group at 24, 36, 48, 72, and 96 h were recorded as 0.619, 0.602, 0.605, 0.604, and 0.624, respectively, while Y(II) values were 0.583, 0.566, 0.554,

0.558, and 0.586, respectively. In comparison, the control group exhibited Fv/Fm values of 0.628, 0.626, 0.627, 0.655, and 0.659, and Y(II) values of 0.595, 0.582, 0.594, 0.614, and 0.618, respectively. The OJIP curve depicts the instantaneous fluorescence intensity change from 0 to 1 s after *N. gaditana*' PSII receives an external saturation pulse. Following the J phase, the fluorescence values in the experimental group notably lagged behind those of the control group after RAP treatment. Moreover, the performance of the experimental group in the I and P phases tended to plateau. Consequently, the primary electron response performance of PSII in the control group significantly surpassed that of the experimental group (Fig. 3B). These findings suggest that inhibition of

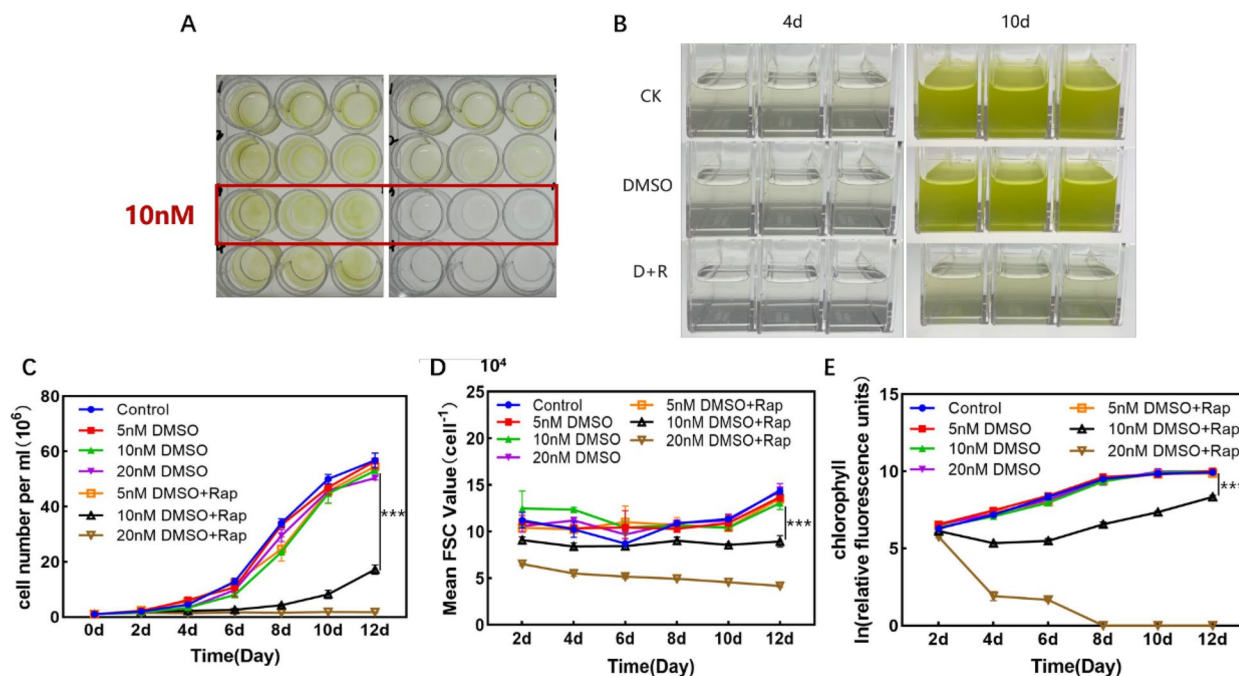


Fig. 2 Growth phenotypes of *N. gaditana* under varying concentrations of RAP. **A** Concentration screening of RAP. Algal cell growth was assessed under treatment concentrations of 0, 5, 10, 20, 30, 40 and 50 nM. **B** Growth status post-RAP treatment on day 4 and day 10 after expanded culture. **C** Growth curves following treatment with selected RAP concentrations of 5, 10 and 20 nM. **D** FSC Value after treatment with varying concentrations of RAP (5, 10, 20 nM). **E** Chlorophyll fluorescence values following treatment with varying concentrations of RAP (5, 10, 20 nM). CK denotes the WT group without treatment, DMSO indicates the control group treated with the solvent DMSO, and D+R represents the experimental group treated with RAP (equivalent to DMSO + RAP below). ***, p -value < 0.001. Error bars represent the standard error of the mean ($n = 3$)

the TOR signaling pathway can lead to defects in photosynthetic autotrophic growth in *N. gaditana*.

Light-response curves are commonly used to assess adaptation to varying light intensities. In this experiment, we determined the rETR of PSII during the initial 6 h, the second day, and the midpoint of the photoperiod on the third day of incubation (54 h, 78 h), and generated a light-response curve through curve fitting (Fig. 3C). Our findings revealed no significant change in rETR after the initial 6-h treatment. However, as the treatment duration increased, a significant decrease was observed after incubation until the midpoint of the photoperiod on the second day (54 h), with a further strengthening of the inhibitory effect observed after the midpoint of the photoperiod on the third day (78 h). These results indicate that the TOR signaling pathway exerts regulatory control over photosynthesis in *N. gaditana*.

TOR signaling on chloroplast morphology and lipid accumulation in *Nannochloropsis gaditana*

Chloroplast formation and development are essential molecular processes for photosynthetic organisms, including algae and plants, to achieve photosynthetic autotrophy, serving as the foundation of algal

photosynthesis. To investigate whether the impairment of photosynthetic autotrophy due to TOR inhibition is linked to chloroplast production, we examined and analyzed chloroplast morphology and development under TOR inhibition using transmission electron microscopy in normally growing and TOR-inhibited algal cells. The results indicated that algal cells maintained a complete chloroplast structure after 3 days in standard culture conditions (ASW + F/2). In contrast, under TOR-inhibited conditions (ASW + F/2 + 10 nM RAP) for the same duration, the cells exhibited no discernible chloroplast morphology. Instead, numerous starch granules (black arrowheads) and variously shaped lipid droplets (white arrowheads) were observed (Fig. 4A). Starch granules, which are energy storage structures within chloroplasts, facilitate algal growth and contribute to plastid transformations such as chloroplast development. Damage to the chloroplast structure impairs chlorophyll synthesis, leading to a significant reduction in chlorophyll content to 0.73 mg/L after 3 days of RAP treatment—a fourfold decrease from the control (Fig. 4B).

The results demonstrated that reduced TOR activity not only impairs chlorophyll synthesis but also alters chloroplast structure, including the complete

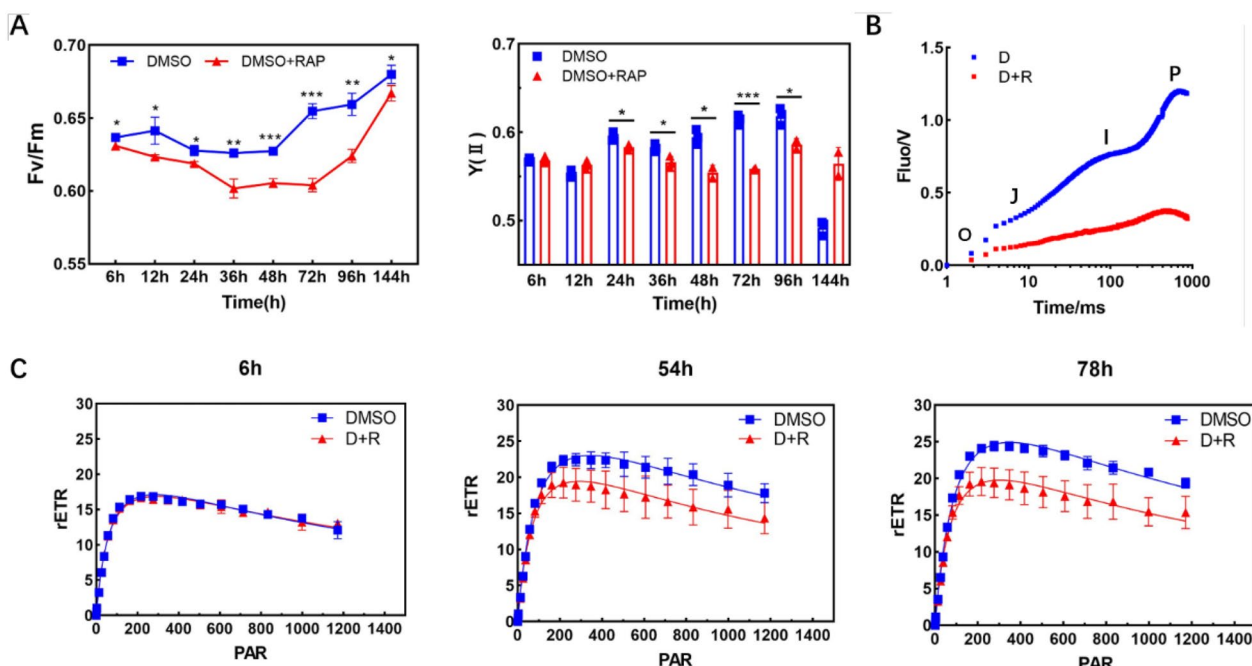


Fig. 3 Photosynthetic characteristics after RAP treatment. **A** Fv/Fm and Y(II) after RAP (10 nM) treatment. **B** OJIP curve after 72 h of RAP (10 nM) treatment. **C** rETR of 6 h, 54 h and 78 h of RAP (10 nM) treatment. DMSO indicates the control group treated with the solvent DMSO, while DMSO + RAP denotes the experimental group treated with RAP. *, p -value < 0.05, **, p -value < 0.01, ***, p -value < 0.001. Error bars represent the standard error of the mean ($N=3$)

disappearance of the basal endocyst membrane and a reduction in cellular grain size (Fig. 4C). On the other hand, RAP treatment induced the accumulation of intracellular lipids (Fig. 4D). The quantitative results showed that the lipid productivity reached 3.25 mg/L/day after 96 h of RAP treatment, significantly higher than that of the control group (Fig. 4E). This suggests that the inhibition of photosynthetic autotrophy by RAP treatment disrupted energy conversion, leading to lipid accumulation. These findings indicate that the TOR signaling pathway plays a crucial role in regulating chlorophyll synthesis and lipid metabolism in *N. gaditana*, which significantly impacts the photosynthetic autotrophy of the algae. Moreover, TOR inhibition contributes to the observed changes in chloroplast morphology, suggesting extensive chloroplast damage.

Effects on TOR signaling under the action of the photosynthesis inhibitor DCMU

Dichlorophenyl dimethylurea (DCMU), commonly known as diuron, is a synthetic photosynthesis inhibitor known for its high specificity and sensitivity. It binds to the QB binding site in the reaction center of Photosystem II (PS II), disrupting electron transfer from QA to QB. Various concentrations of DCMU (3-(3,4-dichlorophenyl)-1,1-dimethylurea) were

administered to treat *N. gaditana*, with concentrations set at 0.05 μ M, 0.2 μ M, 0.4 μ M, 0.6 μ M, and 0.8 μ M. The results indicated inhibition of algal cell growth at a concentration of 0.05 μ M, accompanied by significant reductions in both Fv/Fm and Y(II) values, reflecting an evident inhibition of photosynthesis (Fig. 5A). Specifically, the Fv/Fm values were 0.647 in the wild type and 0.531 in the DCMU-treated algal cells, significantly lower ($p < 0.05$) than those of the wild type. Similarly, the Y(II) values were 0.610 in the wild type and 0.170 in the DCMU-treated algal cells, also significantly lower ($p < 0.05$) than those of the wild type at 48 h (Fig. 5B). The preceding findings demonstrate that exogenous DCMU at a concentration of 0.05 μ M significantly inhibits photosynthesis in *N. gaditana*. The expression of key genes related to the TOR signaling pathway in *N. gaditana* was quantitatively analyzed using fluorescence-based quantitative PCR. The differences in the expression of genes within the TOR protein complex were used to explore the potential impact of photosynthesis inhibition following DCMU treatment on TOR complex gene expression, which, in turn, could affect the function of the TOR signaling pathway. The results revealed that after 48 h of DCMU treatment, the transcript levels of genes involved in the TOR signaling complex were significantly down-regulated in *N. gaditana* (Fig. 5C). This down-regulation

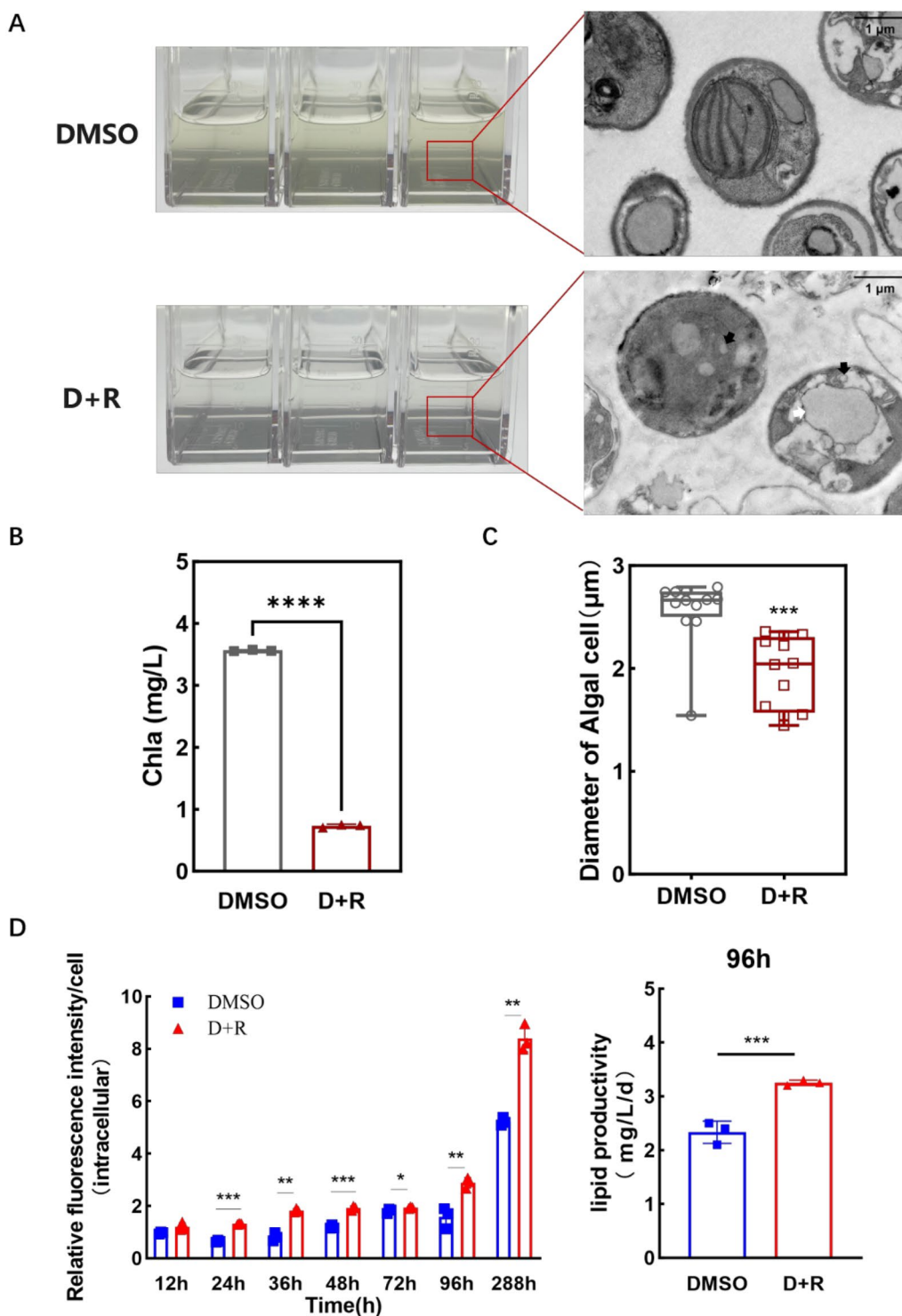


Fig. 4 Impact of RAP treatment on chloroplast development. **A** Transmission electron microscopy of RAP treatment on day 3. White arrows point to lipid droplets and black arrows to starch granules. **B** Chlorophyll content of RAP treatment on day 3. **C** The diameter of single cells from 3 days of RAP treatment. **D** Characterization of relative lipid content in RAP-treated single cells using Nile-Red staining and lipid productivity on 96 h after RAP treatment. DMSO indicates the control group treated with the solvent DMSO, and D+R represents the experimental group treated with RAP. *, p -value < 0.05, **, p -value < 0.01, ***, p -value < 0.001, ****, p -value < 0.0001. Error bars represent the standard error of the mean ($n=3$)

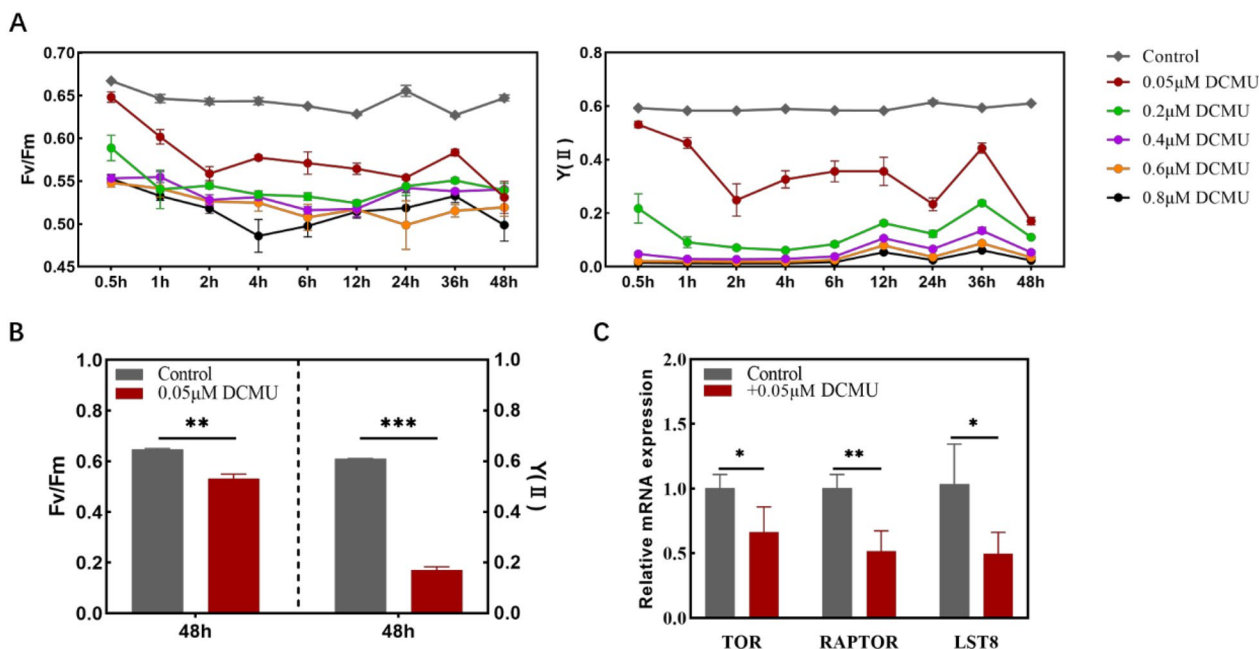


Fig. 5 Impact of the photosynthesis inhibitor DCMU on TOR signaling. **A** Fv/Fm and Y(II) values were measured after treatment with varying DCMU concentrations (0.05, 0.2, 0.4, 0.6, and 0.8 μM). Samples were collected at 0.5, 1, 2, 4, 6, 12, 24, 36, 48 h post-treatment. **B** Fv/Fm and Y(II) values after 48 h of treatment with 0.05 μM DCMU. **C** Expression levels of *TOR*, *RAPTOR* and *LST8* after 48 h of treatment with 0.05 μM DCMU. *, p -value < 0.05, **, p -value < 0.01, ***, p -value < 0.001. Error bars represent the standard error of the mean ($n=3$)

suggests that photosynthesis inhibition by DCMU leads to a comprehensive reduction in the expression of TOR complex genes, thereby affecting the functionality of the TOR signaling pathway. These findings provide evidence of a regulatory link between TOR signaling and photosynthesis in *N. gaditana*.

Transcriptome analysis of targeted metabolic pathways regulated by TOR inhibition in *Nannochloropsis gaditana*

To investigate the molecular interactions between the TOR signaling pathway and photosynthetic growth in *N. gaditana*, both wild type and RAP-treated specimens were employed as experimental subjects. Transcriptome sequencing (RNA-seq) was utilized to examine variations in gene expression, elucidating the role of the TOR signaling pathway when inhibited by RAP.

This study's transcriptome annotation utilized the *N. gaditana* reference genome (NCBI species classification number: 72520), identifying 10,225 genes, comprising 9,616 known and 309 predicted novel genes. The reference genome comparison rate was 91.19%, indicating both ample sequencing data and high-quality sequencing (Supplementary Table S2). Samples were collected over one light–dark cycle at four time points: 6 h (ZT18), 12 h (ZT24), 18 h (ZT30), and 24 h (ZT36) for both the experimental (+RAP) and control groups (Fig. 6A). Principal component analysis (PCA) of the transcriptome samples

revealed tight clustering within groups, demonstrating excellent experimental reproducibility, and clear differentiation between groups (Supplementary Figure S2). This analysis establishes a robust dataset for exploring differential gene expression between light and dark cycles. Differential gene counts were 1958, 917, 5086, and 6496 at the respective time points, with over 50% being significantly down-regulated in each interval (Supplementary Figure S2). To ensure the accuracy of the transcriptome data, 14 DEGs were randomly selected for quantitative real-time PCR (qRT-PCR) analysis. The qRT-PCR findings mirrored the trends observed in the transcriptome data (Supplementary Figure S3), validating its authenticity and reliability.

Six hours post-treatment (ZT18), sequencing identified 1958 differentially expressed genes (DEGs), with 902 up-regulated and 1056 down-regulated. Twelve hours post-treatment (ZT24), 917 DEGs were found, comprising 394 up-regulated and 523 down-regulated genes. These DEGs were classified by Gene Ontology (GO) terms, with the top 28 significantly enriched terms primarily concentrating on molecular functions (14 terms), biological processes (12 terms), and cellular components (2 terms). GO enrichment analysis highlighted Ribosome and Structural constitute of ribosome as the most significantly enriched DEGs, demonstrating the TOR signaling pathway's conservative role in ribosome biosynthesis in *N. gaditana*

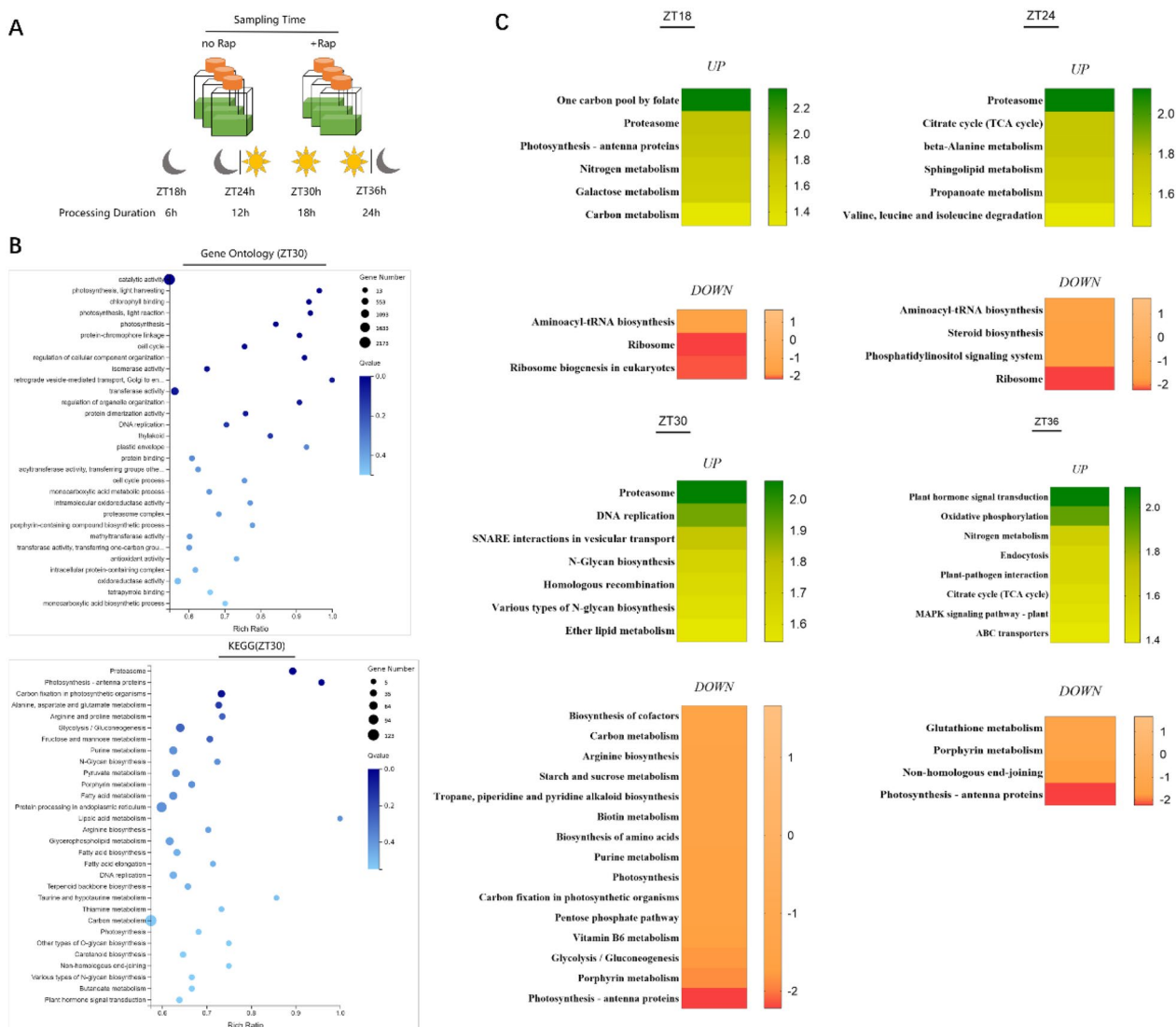


Fig. 6 Transcriptome analysis of *N. gaditana* during one light–dark period following RAP treatment. **A** Transcriptome sampling time points: four time points (6, 12, 18, and 24 h) after RAP treatment were selected and labeled as ZT18, ZT24, ZT30, and ZT36, respectively. **B** GO and KEGG enrichment analysis at photoperiod ZT30. **C** Heatmap of Gene Set Enrichment Analysis (GSEA) for the entire light–dark cycle

(Supplementary Figure S4). Additionally, cellular component GO terms revealed terms associated with plastid formation and chloroplast.

Between 18 to 24 h post-treatment, cells transitioned into the photoperiod, revealing 5086 and 6496 differentially expressed genes (DEGs), with 2450 and 3266 genes up-regulated, and 2636 and 3230 genes down-regulated, respectively. Significant Gene Ontology (GO) terms, highlighted key biological processes associated with photosynthesis and chloroplast development, including light harvesting, chlorophyll binding, and light reactions. KEGG pathway analysis identified several pathways implicated in photosynthesis, notably

“photosynthesis-antenna proteins” and “Carbon fixation in photosynthesis” (Fig. 6B). Further examination of differentially expressed genes (DEGs) indicated a significant down-regulation of genes associated with photosynthesis, predominantly affecting light and dark reactions, as well as chlorophyll biosynthesis. This implies that the TOR signaling pathway plays a crucial role in various metabolic processes, including photosynthesis, chlorophyll biosynthesis, and the metabolism of sugars and lipids.

When individual gene changes are subtle, screening for differentially expressed gene enrichment based on a specified threshold value in differential pathways yields

variable results due to the diversity in threshold settings. Gene Set Enrichment Analysis (GSEA) addresses the limitations of traditional enrichment analysis in extracting information from genes with minor effects, offering a more comprehensive examination of pathway regulation. By employing GSEA to evaluate the Normalized Enrichment Score (NES) of the KEGG pathway across sample groups, a higher absolute NES value signifies considerable biological importance of the pathway's gene set under experimental conditions. The results indicated that, 6 h after the initial treatment (ZT18), nine pathways were significantly enriched. Of these, six pathways were up-regulated ($NES > 1$, $p < 0.05$, $FDR < 0.25$), while three pathways were down-regulated ($NES < 1$, $p < 0.05$, $FDR < 0.25$). At 12 h after the initial treatment (ZT24), ten pathways were significantly enriched. Of these, six were up-regulated ($NES > 1$, $p < 0.05$, $FDR < 0.25$), while four were down-regulated ($NES < 1$, $p < 0.05$, $FDR < 0.25$). Between 18 and 24 h post-treatment (ZT30 and ZT36), during the photoperiod, 22 and 12 differential pathways were enriched, respectively. At ZT30, seven pathways were significantly up-regulated ($NES > 1$, $p < 0.05$, $FDR < 0.25$) and three were significantly down-regulated ($NES < 1$, $p < 0.05$, $FDR < 0.25$). At ZT36, eight pathways were significantly up-regulated ($NES > 1$, $p < 0.05$, $FDR < 0.25$), and four were significantly down-regulated ($NES < 1$, $p < 0.05$, $FDR < 0.25$).

The down-regulated pathways enriched by NES values from 6 to 12 h post-treatment primarily included ribosome biosynthesis, aminoacyl-tRNA biosynthesis, steroid biosynthesis, and the phosphatidylinositol signaling system. The most significantly up-regulated pathways were the proteasome, sphingolipid metabolism, nitrogen metabolism, galactose metabolism, carbon metabolism, and TCA cycle. Between ZT30 and ZT36, cells entered the photoperiod, during which down-regulated pathways were enriched based on NES values. These included porphyrin metabolism, photosynthesis-antenna proteins, photosynthesis, photosynthetic carbon fixation, amino acid biosynthesis, carbon metabolism, glycolysis/glycogenesis, and starch and sucrose metabolism. up-regulated pathways included DNA replication, SNARE interactions in vesicular transport, phytohormone signaling, oxidative phosphorylation, nitrogen metabolism, plant-pathogen interactions, TCA cycle, and MAPK signaling pathway in plants. The results indicated that ribosome biosynthesis, steroid biosynthesis, and phosphatidylinositol signaling were down-regulated during the pre-TOR signaling inhibition period. Metabolic pathways related to photosynthesis and basal substance metabolism were significantly down-regulated upon entering the photoperiod under TOR signaling inhibition, whereas pathways involved in environmental responses and defense mechanisms were

activated. This suggests that during the pre-TOR signaling inhibition period, energy supply, protein homeostasis, membrane integrity, and intracellular signaling are compromised. Moreover, inhibition of TOR signaling further disrupts photosynthesis-related pathways and affects nutrient metabolism and allocation after the onset of the photoperiod. This also indicates that the TOR signaling pathway regulates the relationship between photosynthesis and nutrient partitioning in *N. gaditana*, and that this regulation occurs through a signaling cascade.

TOR signaling in *Nannochloropsis gaditana*: regulating photosynthesis and nutrient energy partitioning

RAP primarily inhibits the TORC1 complex, which regulates photosynthesis, chlorophyll synthesis, and the metabolism of amino acids, sugars, and lipids in *N. gaditana*. In this study, we examined the impact of TOR inhibition on photosynthesis and metabolic pathways in *N. gaditana* by specifically targeting TOR activity with RAP.

The results showed that most genes associated with photosynthesis were significantly down-regulated after 18 h of treatment, when the cells entered the photoperiod. These genes were primarily involved in photosynthesis, photosynthetic carbon fixation, porphyrin metabolism, and chlorophyll biosynthesis. Among them, light-response-related genes encoding the light-harvesting protein complex and chlorophyll a/b-binding proteins (e.g., *LHCA1*, *LHCA2*, and *LHCB2*) were significantly down-regulated (Fig. 7A). Additionally, genes related to the photosystem II core complex (*psb27*, *psbO*, *psbQ*, *psbM*, *psbS*, and *psbU*) and electron transfer (*petF*, *petH*, and *petJ*) also exhibited a down-regulation trend. Furthermore, the expression of *atpG*, an F-type ATP synthase-related gene, was reduced (Fig. 7B). The data suggest that RAP treatment impairs the function of photosystem II and electron transport by inhibiting TOR activity. In the downstream carbon metabolism of photosynthesis, the Calvin cycle plays a central role as the primary pathway for carbon fixation. The results showed a significant down-regulation in the expression of rate-limiting enzyme genes involved in the carbon metabolism pathway (e.g., *PGK*, *PPGK*, *GAPDH*, *TPI*, *SBP*, *ALDO*, *rpe*, and *FBP*) (Fig. 7C). These changes in gene expression indicate that TOR inhibition may disrupt key steps in carbon metabolism, thereby reducing carbon fixation efficiency, which in turn limits photosynthetic rate and cell growth.

Chlorophyll plays a central role in photosynthesis by absorbing light energy and facilitating electron transfer. In the porphyrin metabolic pathway, this study found a significant down-regulation of 12 differentially expressed genes involved in chlorophyll biosynthesis, including

chlorophyll A synthase (*chlG*), protochlorophyll reductase (*por*), 8-vinyl reductase (*DVR*), and magnesium-protoporphyrin methyltransferase (*chlM*) (Fig. 7D). These findings further suggest that TOR inhibition negatively impacts chlorophyll biosynthesis. Additionally, CO₂ is assimilated into glycerol 3-phosphate (G3P) through the Calvin cycle under light-driven conditions, and the fate of G3P determines the allocation of organic carbon. In this study, we observed an up-regulation in the expression of genes related to glycolysis, fatty acid synthesis, fatty acid elongation, and unsaturated fatty acid synthesis under TOR inhibition (Fig. 7E). These changes suggest that TOR inhibition may redirect metabolic flow, with more carbon being diverted toward starch and lipid synthesis pathways, thereby promoting energy storage.

Transcriptome analysis revealed that NgTOR significantly affects photosynthesis in *N. gaditana*. Most genes associated with photosynthesis were significantly down-regulated. Specifically, genes involved in the “photosynthesis,” “photosynthetic antenna proteins,” and “photosynthetic carbon sequestration” pathways were enriched in 16, 21, and 26 genes, respectively. Additionally, genes related to photosystem II and chlorophyll a/b-binding proteins were significantly down-regulated under NgTOR inhibition (Supplementary Table S3). Additionally, all 28 chlorophyll synthesis genes in the “porphyrin-chlorophyll biosynthesis” pathway were down-regulated by 0.53- to 2.56-fold (Supplementary Table S3). Down-regulation of NgTOR also led to the decreased expression of key enzyme genes in the TCA cycle, resulting in reduced energy supply and, consequently, inhibited cell growth. In summary, several genes involved in photosynthesis, chlorophyll biosynthesis, and carbon metabolism were significantly down-regulated, while genes associated with glycolysis and lipid synthesis showed an up-regulation trend in algal cells after 18 h of RAP treatment. These findings suggest that the TOR signaling pathway, functioning as a central regulator, may coordinate photosynthetic growth and metabolic allocation by modulating photosynthesis and downstream energy and nutrient metabolism pathways. Additionally, TOR may act as a crucial “switch” in regulating both photosynthetic growth and lipid accumulation in *N. gaditana*.

Material and methods

Strains and culture conditions

Nannochloropsis gaditana CCMP 526, was a kind gift from Danxiang Han (Institute of Hydrobiology, Chinese Academy of Sciences). This microalga was cultivated in artificial seawater prepared using Fauna Marin salts (Holzgerlingen, Germany) and supplemented with f/2 nutrient medium (catalog number G0154, Sigma-Aldrich, MO, USA). The cultures were maintained in

sterile, gas-permeable square flasks with a surface area of 175 cm² (Corning®, Corning, NY, USA), each containing 100 mL of the prepared growth medium.

In the rapamycin (RAP) concentration gradient experiment, the following concentrations were tested: 0 nM, 5 nM, 10 nM, 20 nM, 30 nM, 40 nM, and 50 nM. The cultures were incubated under these conditions, with an initial *N. gaditana* cell density standardized to 1 × 10⁶ cells/mL to ensure consistency across samples. Experimental treatments were performed in triplicate to ensure the reliability and reproducibility of results. The atmospheric carbon dioxide concentration was maintained at 1.5% (by volume), and the cultures were exposed to an irradiance of 50 μmol photons m⁻² s⁻¹ under a 12-h light/12-h dark photoperiod. The incubation temperature was kept constant at 22 °C to optimize growth conditions.

Cell growth

Cell growth was analyzed by measuring cell density (in cells/mL) and dry cell weight (DCW). Cells were inoculated at 10⁶ cells/mL, determined using CytoFLEX S flow cytometer (Beckman, Brea, CA, USA). The sample was quantified by CytoFLEX S flow cytometer (Beckman, Brea, CA, USA) using a fluorescence channel with excitation light at 488 nm and emission light at 685 nm to quantify the concentration of *N. gaditana* CCMP526 cells. Chlorophyll fluorescence data were analyzed using two-way ANOVA (GraphPad Prism 8.4, 2020, Boston, MA, USA).

Determination of lipid content and lipid productivity in individual cells

The lipid content of individual algal cells was quantified by flow cytometry, enabling the measurement of fluorescence intensity. The measurements were conducted with an excitation wavelength of 488 nm and an emission wavelength of 575 nm. To prepare the samples, 1 mL of the algal culture was collected and subsequently combined with 50 μL of dimethyl sulfoxide (DMSO) as an osmotic agent and 2 μL of Nile Red stain (0.5 mg/mL). The resulting mixture was thoroughly homogenized and incubated in the dark for over 40 min to ensure optimal staining.

Algal cells were collected after 96 h of culture. Then, 8 mL of a chloroform–methanol–water mixture (v/v = 2:1:1) was added, and the mixture was placed in a water bath shaker at 35 °C (150 rpm) for overnight incubation. The sample was then centrifuged at 8000 rpm for 10 min, resulting in three distinct layers: the upper layer containing the aqueous methanol–water phase, the middle layer consisting of algal biomass, and the lower chloroform phase containing oil and lipids. The lower chloroform phase was carefully collected, and the upper

aqueous phase was discarded. The extraction of the middle algal biomass layer was repeated twice. After drying and weighing the glass test tube, the chloroform phase collected from all three extractions was combined, nitrogen was passed through to remove any remaining solvents, and the final weight was measured to calculate the mass of oil.

Chlorophyll fluorescence analysis

The chlorophyll fluorescence of *N. gaditana* was analyzed using a MULTI-COLOR-PAM fluorometer (Walz, Germany) and PAMWin3 software. Algal cells were treated with 10 nM RAP and collected by centrifugation at 6, 12, 24, 36, 48, 72, 96, 144 h post-treatment. The maximum photochemical efficiency (F_v/F_m) and the actual photosynthetic quantum yield ($Y(II)$) were measured during light energy conversion in the chloroplast PSII light-harvesting antenna. The relative electron transfer rate (rETR) was analyzed by collecting algal cells at 6, 54, and 78 h after treatment, while the OJIP curve was measured at 72 h. These measurements were conducted to investigate whether the TOR signaling pathway regulates photosynthesis in algal cells.

A subset of algal samples from the batch culture was diluted to achieve a chlorophyll content of approximately 200 $\mu\text{g/L}$ and then incubated in the dark for 20 min. Prior to utilization, the apparatus was calibrated to zero, and the Ft was adjusted to 1.5 in advance of measurement. The measurements were conducted with a 440 nm measuring light and white light as actinic light, in accordance with the incubation conditions. A 1.5-mL sample was placed in a 10-mm cuvette and the minimum fluorescence (F_o) was recorded in the absence of light. The maximum fluorescence (F_m) was obtained by applying a 3000 $\mu\text{mol photons m}^{-2} \text{s}^{-1}$ saturating flash. In the case of light-adapted states, actinic light was applied with saturating pulses every 20 s, capturing steady-state fluorescence (F) and maximum light-adapted fluorescence (F_m'). The formulas for F_v/F_m and $Y(II)$ were then applied to calculate the respective efficiencies. The calculations for F_v/F_m and $Y(II)$ employed the formulas

$$F_v/F_m = (F_m - F_o)/F_m \text{ and } Y(II) = (F_m' - F)/F_m'$$

The OJIP assay measures the fluorescence rise in the kinetic curve, conducted under fast trigger conditions. Initially, the system was set to the fast trigger mode using the sigma1000. FTM file, with ML activated just 100 μs prior to AL initiation. Fluorescence readings were then collected at 10- μs intervals, documenting the entire process over 1 s. This setup ensured precision in capturing the rapid fluorescence changes.

The relative electron transfer rate (rETR) and the fast photoresponse curve of Photosystem II were determined

by setting the measurement light wavelength to 440 nm, setting 20 steps (0, 2, 3, 14, 26, 38, 57, 82, 113, 162, 217, 276, 348, 418, 505, 607, 713, 833, 999, 1172 $\mu\text{mol m}^{-2} \text{s}^{-1}$). White light at the wavelength of 420–640 nm was used as the photochemical light, with a duration of 20 s per shift and a saturation pulse (duration of 800 ms) turned on at the end of each shift. The relative electron transfer rate (rETR) for each light intensity was determined using the equation $\text{rETR(II)} = Y(II) \times \text{PAR} \times 0.5$. Here, $Y(II)$ represents the effective photon yield from the equation, PAR denotes the photochemical light intensity (in $\mu\text{mol photons m}^{-2} \text{s}^{-1}$), and the factor 0.5 assumes an equal distribution of absorbed photons between Photosystem I and II. The rETR values were modeled based on the equation $\text{rETR} = \text{PAR}/(a \times \text{PAR}^2 + b \times \text{PAR} + c)$, where PAR is the specified photochemical light intensity, and a , b , and c are fitting parameters [36, 37].

Transmission electron microscopy analysis

Samples were collected at the end of the photoperiod on day 3 of the batch culture. *N. gaditana* cells underwent centrifugation at 3000 $\times g$ for 5 min, followed by resuspension in 0.1 M phosphate buffer (pH 7.4) with 4% glutaraldehyde added. They were fixed overnight at 4 °C in the dark. The Xiamen University Biomedical Instrument Sharing Platform conducted sample preparation and sectioning. High-resolution transmission electron microscopy (TEM) images were acquired using a Hitachi HT-7800 transmission electron microscope at 100 kV. ImageJ software was used to select 15 intact cells from each sample for size analysis, based on the TEM images.

Determination of chlorophyll content

To obtain algal cells, an adequate volume of algal liquid was filtered using a sandwich filter setup, depositing the cells onto a 0.45- μm GF/F membrane ($\Phi 25$ mm, Whatman). The filter membrane was then fully submerged in 4 mL of anhydrous methanol and left to extract overnight at 4 °C in darkness until the green coloration on the membrane was no longer discernible. Subsequently, an appropriate volume of the extracted solution was centrifuged at 18,000 $\times g$ for 5 min to eliminate insoluble impurities. From this purified solution, 1.2 mL was extracted as the sample for measurement. Following the protocol outlined by Porra, a spectrophotometer was employed to determine the absorbance value, facilitating the calculation of chlorophyll a concentration using the prescribed formula: $\text{Chl a } (\mu\text{g mL}^{-1}) = 16.29 \times (A_{665.2} - A_{750}) - 8.54 \times (A_{652} - A_{750})$.

RNA-seq sample preparation

To ensure the efficient isolation of algal cells, the culture was promptly filtered through a 0.4- μm polycarbonate

membrane (Millipore, Isopore™, Billerica, USA) using a vacuum-driven filtration apparatus (Millipore, Strifil®, Billerica, USA). Algal cells retained on the filter were carefully resuspended in 2 mL of phosphate-buffered saline (PBS) and transferred into a 2-mL sterile grinding tube. The samples were then centrifuged at 5000×g for 5 min at 4 °C to pellet the cells. Following centrifugation, the supernatant was removed, and the algal pellet was immediately flash-frozen in liquid nitrogen to preserve RNA integrity. The frozen cell pellet was subsequently transferred to a pre-cooled grinding device, where two sterile stainless-steel beads, pre-chilled to minimize thermal degradation, were added. The cells were homogenized at a frequency of 55 Hz for 30 s to ensure thorough disruption of cell structures.

To the homogenized sample, lysis buffer from the RNA extraction kit (GeneBetter®, Beijing, China) was added according to the manufacturer's guidelines, and the mixture was vortexed vigorously for 20 s to facilitate complete lysis and RNA release. Total RNA was extracted from the disrupted *N. gaditana* cells following the protocol provided with the RNA extraction kit. The purity and concentration of the extracted RNA were quantitatively measured using a NanoDrop 2000 spectrophotometer (Thermo Fisher Scientific, Wilmington, DE, USA). The RNA's structural integrity was evaluated using the RNA Nano 6000 Assay Kit with an Agilent Bioanalyzer 2100 system (Agilent Technologies, Santa Clara, CA, USA), providing high-resolution quality assessment critical for downstream RNA-seq applications.

Constructing sequencing libraries for transcriptome studies

For transcriptome library preparation, 1 µg of RNA per sample was utilized. Libraries were constructed using the Hieff NGS Ultima Dual-mode mRNA Library Prep Kit for Illumina (Yeasen Biotechnology, Shanghai, China) according to the manufacturer's protocol, with unique index codes assigned to each sample. Briefly, mRNA was isolated from total RNA using poly-T oligo-coated magnetic beads. First-strand cDNA synthesis was followed by second-strand synthesis to create double-stranded cDNA. Enzymatic treatments converted overhangs into blunt ends, and 3' adenylation was performed to facilitate adaptor ligation using NEBNext Adapters with hairpin loop structures.

The resulting fragments were purified using the AMPure XP system (Beckman Coulter, Beverly, USA). Adaptor-ligated cDNA was treated with USER enzyme (NEB, MA, USA) at 37 °C for 15 min, followed by inactivation at 95 °C for 5 min. PCR amplification was then carried out using Phusion High-Fidelity DNA polymerase with universal and index primers. The amplified products

were purified again with the AMPure XP system, and the final library quality was assessed using an Agilent Bioanalyzer 2100 system to ensure suitability for sequencing.

Transcriptome assembly, annotation, and differential expression analysis

The raw reads were processed using the BMKCloud bioinformatics pipeline tool on the online platform (www.biocloud.net). Initially, raw data in fastq format underwent processing via custom Perl scripts, resulting in clean data by eliminating adapter sequences, poly-N sequences, and low-quality reads. Concurrently, quality metrics such as Q20, Q30, GC content, and sequence duplication levels were assessed for the clean data. Subsequent analyses relied solely on this high-quality clean data. Adaptor sequences and low-quality reads were removed to refine the datasets further. The reference gene set, derived from the annotated *N. gaditana* B-31 genome (<http://www.nannochloropsis.org/page/ftp/>), served as the basis for further analysis and annotation of reads, allowing only those with a perfect match or a single mismatch.

The Hisat2 software was utilized for mapping against the reference genome. Gene annotation was performed with the use of multiple databases, including the NCBI non-redundant proteins database (Nr), the Protein Families database (Pfam), the Clusters of Orthologous Groups database (KOG/COG), the curated protein sequences database (Swiss-Prot), the KEGG Orthology database (KO), and the Gene Ontology database (GO). The differential gene expression was analyzed using DESeq2, which applies statistical modeling based on the negative binomial distribution. The enrichment analysis of the differentially expressed genes (DEGs) was conducted with the KEGG KOBAS database and the clusterProfiler package, with the objective of identifying significant pathways. Additionally, a GO enrichment analysis was performed via clusterProfiler, with the aim of correcting for potential biases using the Wallenius non-central hyper-geometric distribution.

RNA extraction and quantitative real-time PCR

The microalgal samples were collected using 0.4-µM PCM (Millipore, Isopore™, Billerica, USA) filtered through an extraction flask (Millipore, Strifil®, Billerica, USA), eluted with 2 mL PBS buffer into a 2-mL grinding tube, centrifuged 5000×g for 5 min at 4 °C, the supernatant was discarded and then immediately frozen in liquid nitrogen. The frozen algae and pre-cooled sterile steel beads were placed in a freezer grinder for 30 s at 55 Hz. After grinding is complete, total RNA is extracted from samples using the RNA extraction kit (GeneBetter®, Beijing, China). We confirmed the expression levels of the target genes through Quantitative real-time PCR with

specific primers, and assessed gene expression detailed in Supplementary Table S4. The universally conserved actin gene served as the internal reference for normalization.

Methodological approach to statistical evaluation

The study employed a structured methodology, incorporating biological and technical replicates, and a statistical evaluation of the collected data. To ensure reliability and reproducibility of the observed patterns and correlations, each growth condition was investigated using two independent biological replicates, each accompanied by three technical replicates. For each data point, the mean of the technical replicates was calculated. This consistent approach was implemented across enzyme activity measurements and related experimental procedures.

For the purposes of statistical analysis, the technical replicate data from each biological replicate were combined and analyzed using ANOVA. The error bars illustrate the standard deviation of the mean, which was calculated from three replicates. The differences among the treatments were assessed through Tukey's test, with a significance level of $p < 0.05$. All statistical computations were carried out using GraphPad Prism software (GraphPad Prism 8.4, 2020, Boston, MA, USA), with two-way ANOVA as the analytical method.

Discussion

TOR proteins play a pivotal role in the growth and development of both photosynthetic and non-photosynthetic eukaryotes. The TOR regulatory network is involved in nutrient and energy signaling, as well as transcription and regulation of multiple signaling pathways. However, the extent to which TOR influences chloroplast development and photosynthetic signaling in *N. gaditana*, along with the underlying molecular mechanisms, remains to be clarified.

In this study, we shed light on the mechanisms by which NgTOR orchestrates multiple cellular functions to regulate cell growth in *N. gaditana*. TORC1, identified in higher plants, the diatom *P. tricornutum*, and the green alga *C. reinhardtii*, comprises crucial proteins: TOR, RAPTOR, and LST8. The activity of TORC1, influenced by nutrients and environmental factors, adapts to varying conditions by modulating intracellular metabolic pathways [23, 34]. In *N. gaditana*, a single conserved NgTOR protein was identified (Fig. 1 and Supplementary Table S1), with TOR, RAPTOR, and LST8 as the core components. Conversely, TORC2 components, RIC-TOR and SIN1, were not detected, implying the presence of a conserved TORC1 pathway in *N. gaditana*. While *C. reinhardtii* exhibits sensitivity to RAP typically at 500 nM [24], our findings reveal that *N. gaditana* exhibits significant growth inhibition at a much lower

RAP concentration of 10 nM (Fig. 2), demonstrating its heightened sensitivity to RAP. Although rapamycin is a valuable tool for studying the TOR signaling pathway, its limitations must be considered. These include its ineffective inhibition of TORC2, variability in specificity across different species and cell types, potential non-specific effects at high concentrations, and the absence of genetic validation, which can lead to incomplete interpretations of results. Therefore, in future studies of the TOR signaling pathway, we will combine genetic tools (e.g., knock-down or RNAi) with other chemical inhibitors to more comprehensively elucidate the role of TOR in cell growth, metabolic regulation, and signal integration.

Interplay between the TOR signaling pathway and photosynthesis in *Nannochloropsis gaditana*

Photosynthesis is a physiological process unique to plants and algae, providing the energy and sugars essential for autotrophic growth [38]. This process distinguishes plants and algae from animals. The TOR signaling pathway is closely linked to chloroplast development and photosynthesis [39, 40]. In both plants and the model alga *C. reinhardtii*, photosynthesis generates ATP and NADPH for CO₂ fixation, which in turn activates TOR, enhancing photosynthetic efficiency [41]. Conversely, DCMU, a photosynthesis inhibitor, down-regulates TOR activity in both algae [41] and plants [42], further highlighting the regulatory role of the TOR pathway downstream of photosynthesis [43].

The interaction between TOR and photosynthesis is complex, and current studies have yet to fully elucidate its regulatory mechanisms [25]. In *C. reinhardtii*, chemical inhibition of TOR disrupts the efficiency of photosystem II (PSII), impairs the state transition between PSII and photosystem I (PSI), and affects the overall photosynthetic process [7]. This suggests that TOR plays an important role in maintaining photosynthetic stability. In this study, our analysis of differentially expressed genes (DEGs) from transcriptomic data revealed that chemical inhibition of TOR significantly impacted the photosynthetic processes in *N. gaditana*, particularly in cyst structure, porphyrin metabolism, and chlorophyll biosynthesis. These changes led to the down-regulation of photosynthesis-related genes and altered the redistribution of downstream carbon metabolic pathways. Additionally, we observed that the expression of TOR signaling pathway-related proteins was suppressed when *N. gaditana* was treated with the photosynthesis inhibitor DCMU. This finding further supports the existence of a reciprocal regulatory relationship between TOR signaling, photosynthesis, and downstream energy allocation. However, it is important to note that the current study relies solely on the results of treatments with

chemical inhibitors (e.g., rapamycin and DCMU), which may have non-specific effects and cannot completely exclude the influence of other pathways on photosynthesis and metabolism. Furthermore, the specific regulatory mechanisms of the TOR signaling pathway remain unresolved, particularly in *N. gaditana* and how TOR signaling coordinates photosystem function, carbon allocation, and metabolic reprogramming requires further investigation using genetic tools (e.g., gene knockout or overexpression).

The TOR signaling pathway modulates nutrient partitioning in photosynthetic downstream processes

The autotrophic nature of green plants within the eukaryotic spectrum is facilitated by the advent and integration of photosynthesis [44], enabling carbon fixation, carbohydrate production, and direct uptake of mineral nutrients like nitrogen, phosphorus, and potassium from the soil. Growth regulation is mediated by the coordination between nutrient acquisition and internal nutrient-sensing signals, notably TOR and AMPK [45, 46]. In photosynthetic organisms, a reduction in TOR signaling typically results in altered amino acid levels [47, 48], decreased sucrose content, and increased accumulation of starch and triacylglycerol, indicating TOR's involvement in carbon (C) and nitrogen (N) signaling and metabolic pathways, as well as their interplay [45, 49, 50]. Supporting evidence from recent research on *C. reinhardtii* reveals that HCO_3^- supplementation as a carbon source for photosynthesis enhances the phosphorylation of RPS6, a downstream target of TOR signaling, reflecting TOR's activity [51–53]. Moreover, the *sta6* mutant exhibited a deficiency in functional ADP-glucose pyrophosphatase, crucial for starch synthesis, resulting in impaired starch production and diminished light absorption capacity. Analysis of RPS6 phosphorylation in *sta6* mutant cells indicated increased TOR activity, implying that starch synthesis inhibition triggers TOR up-regulation, thereby affecting the utilization of fixed carbon during photosynthesis [54, 55]. Overactivation of TOR kinase, as observed through metabolomic analysis, results in increased Gln amino acids levels, suggesting a shift in carbon allocation toward amino acid synthesis over starch synthesis, thereby promoting growth through TOR activation [41, 56]. This highlights the role of the TOR signaling pathway in modulating growth and metabolic pathways via photosynthesis and its by-products [57].

Chemical inhibition of TOR led to increased TAG levels in *C. reinhardtii* and *P. tricornutum*, indicating a conserved mechanism of TAG synthesis regulation across various microalgae species [34, 35, 58]. Nonetheless,

the specific processes through which TOR signaling influences lipid synthesis in microalgae are not well-understood. In our research, we observed a similar lipid accumulation in *N. gaditana* by lipid measurements (Supplementary Figure S5). This observation underscores the potential of TOR inhibition in *N. gaditana* to modulate lipid synthesis alongside growth inhibition, thereby highlighting the significant role of the TOR signaling pathway in regulating photosynthesis and carbon allocation in *N. gaditana*. Further exploration of the precise regulatory networks is warranted.

TOR signaling pathway regulates the balance between photosynthesis and lipid accumulation in *N. gaditana*

The TOR signaling pathway plays a pivotal role in regulating the balance between photosynthesis and lipid accumulation in microalgae, particularly in *N. gaditana* and other model organisms like *C. reinhardtii* and *P. tricornutum*. Studies have demonstrated that TOR integrates environmental signals, such as nutrient availability, and adjusts cellular metabolism to optimize both growth and lipid accumulation. For instance, inhibition of TOR signaling using specific inhibitors like AZD-8055 in *P. tricornutum* has been shown to promote TAG accumulation, while also reducing cell proliferation, highlighting a clear trade-off between biomass production and lipid storage [34]. Similar results were observed in *C. reinhardtii*, where nitrogen starvation and TOR inhibition triggered a massive shift in metabolism, enhancing lipid accumulation while down-regulating photosynthetic activity to conserve energy [51]. Furthermore, research into inositol polyphosphates has uncovered that these molecules interact with TOR to influence carbon metabolism and lipid storage in microalgae [6]. This suggests a complex regulatory mechanism where TOR not only governs growth but also controls how cells allocate resources between photosynthesis and lipid production under stress conditions. In *N. gaditana*, this mechanism is particularly relevant, as the proteomic and transcriptomic shifts associated with lipid accumulation involve extensive down-regulation of photosynthetic activity, confirming that TOR signaling modulates the delicate balance between energy production and storage [59].

In summary, this study provides preliminary evidence for the regulatory role of the TOR signaling pathway in the photosynthesis and energy metabolism of *N. gaditana*. However, some limitations remain. Future studies should integrate genetic and biochemical approaches to further explore the causal relationship between TOR signaling and photosynthesis. These investigations should aim to clarify the specific

mechanisms by which TOR regulates chlorophyll synthesis, maintenance of cyst-like structures, and reprogramming of carbon allocation, thereby advancing our understanding of TOR's role as a central regulator of photosynthetic growth and its molecular basis. Ultimately, by controlling these processes, TOR contributes to cellular homeostasis and survival during nutrient deprivation, with potential applications in biofuel production.

Conclusion

Previous research has established the pivotal role of the TOR signaling pathway in promoting algal growth and lipid production, as well as its significant influence on regulating algal photosynthesis, though the precise mechanisms remain to be elucidated.

In this study, we focused on the TOR signaling pathway in *N. gaditana*, investigating TOR's central role in modulating photosynthesis and growth. We found that RAP effectively inhibited *N. gaditana*'s TOR pathway, resulting in decreased photosynthesis and growth. Additionally, using DCMU to inhibit photosynthesis demonstrated that such suppression also reduced the transcriptional activity of TOR-associated complexes, indicating a bidirectional regulatory relationship. Based on these findings, transcriptome analysis of RAP-treated algal cells in our investigation substantiated that NgTOR governs a range of intracellular metabolic and signaling pathways, primarily influencing photosynthesis, intracellular carbon metabolism, and lipid metabolism pathways. In essence, the TOR signaling pathway in *N. gaditana* is pivotal for photosynthesis, intracellular carbon metabolism, and lipid metabolism, thus providing a basis for further elucidating the mechanisms underlying photosynthetic autotrophy and regulation of lipid metabolism flow distribution in *N. gaditana* as photosynthetic organisms.

Supplementary Information

The online version contains supplementary material available at <https://doi.org/10.1186/s13068-025-02617-6>.

Supplementary Material 1.

Acknowledgements

We wish to thank all members of Zhou Lab for providing valuable suggestions and help during the research.

Author contributions

Conceptualization, Z.Z. (Zhengying Zhang), Y.L. (Yanyan Li) and H.Z. (Hantao Zhou); Data curation, Z.Z. (Zhengying Zhang) and Y.L. (Yanyan Li); Investigation, Z.Z. (Zhengying Zhang) and S.W. (Shuting Wen); Methodology, Z.Z. (Zhengying Zhang) and S.Y. (Shu Yang); Project administration, H.Z. (Hantao Zhou); Supervision, H.Z. (Hongmei Zhu); Writing-original draft, Z.Z. (Zhengying Zhang); Writing-review and editing, H.Z. (Hantao Zhou). All authors have read and agreed to the published version of the manuscript.

Funding

This work was financially supported by the National Natural Science Foundation of China (No. 31371988).

Availability of data and materials

The raw sequence data reported in this paper have been deposited in the Genome Sequence Archive (Genomics, Proteomics & Bioinformatics 2021) in National Genomics Data Center (Nucleic Acids Res 2022), China National Center for Bioinformation/Beijing Institute of Genomics, Chinese Academy of Sciences (GSA: CRA019945) that are publicly accessible at <https://ngdc.cncb.ac.cn/gsa>.

Declarations

Ethics approval and consent to participate

Not applicable.

Consent for publication

Not applicable.

Competing interests

The authors declare no competing interests.

Received: 10 November 2024 Accepted: 3 February 2025

Published online: 22 February 2025

References

- Zabed HM, Akter S, Yun J, Zhang G, Awad FN, Qi X, Sahu JN. Recent advances in biological pretreatment of microalgae and lignocellulosic biomass for biofuel production. *Renew Sustain Energy Rev*. 2019;105:105–28.
- Melis A. Solar energy conversion efficiencies in photosynthesis: Minimizing the chlorophyll antennae to maximize efficiency. *Plant Sci*. 2009;177(4):272–80.
- Sun H, Zhao W, Mao X, Li Y, Wu T, Chen F. High-value biomass from microalgae production platforms: strategies and progress based on carbon metabolism and energy conversion. *Biotechnol Biofuels*. 2018;11:227.
- Song Y, Alyafei MS, Masmoudi K, Jaleel A, Ren M. Contributions of TOR signaling on photosynthesis. *Int J Mol Sci*. 2021;22(16):8959.
- Wu Y, Shi L, Li L, Fu L, Liu Y, Xiong Y, Sheen J. Integration of nutrient, energy, light, and hormone signalling via TOR in plants. *J Exp Bot*. 2019;70(8):2227–38.
- Couso I, Evans BS, Li J, Liu Y, Ma F, Diamond S, Allen DK, Umen JG. Synergism between inositol polyphosphates and tor kinase signaling in nutrient sensing, growth control, and lipid metabolism in *Chlamydomonas*. *Plant Cell*. 2016;28(9):2026–42.
- Upadhyaya S, Rao BJ. Reciprocal regulation of photosynthesis and mitochondrial respiration by TOR kinase in *Chlamydomonas reinhardtii*. *Plant Direct*. 2019;3(11): e00184.
- Swier PB, Mishra H, Lohia R, Saran S. Overexpression of TOR (target of rapamycin) inhibits cell proliferation in *Dictyostelium discoideum*. *J Basic Microbiol*. 2016;56(5):510–9.
- Li L, Zhu T, Huang L, Ren M. Target of rapamycin signaling involved in the regulation of photosynthesis and cellular metabolism in *Chlorella sorokiniana*. *Int J Mol Sci*. 2022;23(13):7451.
- Ingargiola C, Turqueto Duarte G, Robaglia C, Leprince AS, Meyer C. The plant target of rapamycin: a conduct TOR of nutrition and metabolism in photosynthetic organisms. *Genes (Basel)*. 2020;11(11):1285.
- Burkart GM, Brandizzi F. A Tour of TOR complex signaling in plants. *Trends Biochem Sci*. 2021;46(5):417–28.
- Shi L, Wu Y, Sheen J. TOR signaling in plants: conservation and innovation. *Development*. 2018;145(13): dev160887.
- Roustan V, Weckwerth W. Quantitative phosphoproteomic and system-level analysis of tor inhibition unravel distinct organellar acclimation in *Chlamydomonas reinhardtii*. *Front Plant Sci*. 2018;9:1590.
- Brunkard JO. Exaptive evolution of target of rapamycin signaling in multicellular eukaryotes. *Dev Cell*. 2020;54(2):142–55.

15. Calo G, De Marco MA, Salerno GL, Martinez-Noel GMA. TOR signaling in the green picoalga *Ostreococcus tauri*. *Plant Sci.* 2022;323: 111390.
16. Gonzalez A, Hall MN. Nutrient sensing and TOR signaling in yeast and mammals. *EMBO J.* 2017;36(4):397–408.
17. Loewith R, Hall MN. Target of rapamycin (TOR) in nutrient signaling and growth control. *Genetics.* 2011;189(4):1177–201.
18. Dobrenel T, Marchive C, Sormani R, Moreau M, Mozzo M, Montane MH, Menand B, Robaglia C, Meyer C. Regulation of plant growth and metabolism by the TOR kinase. *Biochem Soc Trans.* 2011;39(2):477–81.
19. Jamsheer KM, Jindal S, Sharma M, Awasthi P, Sreejath S, Sharma M, Mannully CT, Laxmi A. A negative feedback loop of TOR signaling balances growth and stress-response trade-offs in plants. *Cell Rep.* 2022;39(1): 110631.
20. Bakshi A, Moin M, Kumar MU, Reddy AB, Ren M, Datla R, Siddiq EA, Kirti PB. Ectopic expression of *Arabidopsis* target of rapamycin (AtTOR) improves water-use efficiency and yield potential in rice. *Sci Rep.* 2017;7:42835.
21. Bakshi A, Moin M, Madhav MS, Datla R, Kirti PB. Target of Rapamycin (TOR) negatively regulates chlorophyll degradation and lipid peroxidation and controls responses under abiotic stress in *Arabidopsis thaliana*. *Plant Stress.* 2021;2: 100020.
22. Montane MH, Menand B. TOR inhibitors: from mammalian outcomes to pharmacogenetics in plants and algae. *J Exp Bot.* 2019;70(8):2297–312.
23. Perez-Perez ME, Couso I, Crespo JL. The TOR signaling network in the model unicellular green alga *Chlamydomonas reinhardtii*. *Biomolecules.* 2017;7(3):54.
24. Crespo JL, Diaz-Troya S, Florencio FJ. Inhibition of target of rapamycin signaling by rapamycin in the unicellular green alga *Chlamydomonas reinhardtii*. *Plant Physiol.* 2005;139(4):1736–49.
25. Werth EG, McConnell EW, Couso Liane I, Perrine Z, Crespo JL, Umen JG, Hicks LM. Investigating the effect of target of rapamycin kinase inhibition on the *Chlamydomonas reinhardtii* phosphoproteome: from known homologs to new targets. *New Phytol.* 2019;221(1):247–60.
26. Juppner J, Mubeen U, Leisse A, Caldana C, Wiszniewski A, Steinhauser D, Gialvalisco P. The target of rapamycin kinase affects biomass accumulation and cell cycle progression by altering carbon/nitrogen balance in synchronized *Chlamydomonas reinhardtii* cells. *Plant J.* 2018;93(2):355–76.
27. Couso I, Perez-Perez ME, Ford MM, Martinez-Force E, Hicks LM, Umen JG, Crespo JL. Phosphorus availability regulates TORC1 signaling via LST8 in *Chlamydomonas*. *Plant Cell.* 2020;32(1):69–80.
28. Diaz-Troya S, Florencio FJ, Crespo JL. Target of Rapamycin and LST8 proteins associate with membranes from the endoplasmic reticulum in the unicellular green alga *Chlamydomonas reinhardtii*. *Eukaryot Cell.* 2008;7(2):212–22.
29. Takeuchi T, Benning C. Nitrogen-dependent coordination of cell cycle, quiescence and TAG accumulation in *Chlamydomonas*. *Biotechnol Biofuels.* 2019;12:292.
30. Pancha I, Tanaka K, Imamura S. Overexpression of a glycogenin, CmGLG2, enhances floridean starch accumulation in the red alga *Cyanidioschyzon merolae*. *Plant Signal Behav.* 2019;14(6):1596718.
31. Ma XN, Chen TP, Yang B, Liu J, Chen F. Lipid production from *Nannochloropsis*. *Mar Drugs.* 2016;14(4):61.
32. Ajjawi I, Verruto J, Aquilino M, Soriaga LB, Coppersmith J, Kwok K, Peach L, Orchard E, Kalb R, Xu W, Carlson TJ, Francis K, Konigsfeld K, Bartalis J, Schultz A, Lambert W, Schwartz AS, Brown R, Moellering ER. Lipid production in *Nannochloropsis gaditana* is doubled by decreasing expression of a single transcriptional regulator. *Nat Biotechnol.* 2017;35(7):647–52.
33. Kilian O, Benemann CS, Niyogi KK, Vick B. High-efficiency homologous recombination in the oil-producing alga *Nannochloropsis* sp. *Proc Natl Acad Sci U S A.* 2011;108(52):21265–9.
34. Prioretti L, Avilan L, Carrière F, Montané MH, Field B, Grégori G, Menand B, Gontero B. The inhibition of TOR in the model diatom *Phaeodactylum tricornutum* promotes a get-fat growth regime. *Algal Res.* 2017;26:265–74.
35. Prioretti L, Carrière F, Field B, Avilan L, Montané MH, Menand B, Gontero B. Targeting TOR signaling for enhanced lipid productivity in algae. *Biochimie.* 2020;169:12–7.
36. Jassby AD, Platt T. Mathematical formulation of the relationship between photosynthesis and light for phytoplankton. *Limnol Oceanogr.* 2003;21(4):540–7.
37. Eilers PH, Peeters JC. A model for the relationship between light intensity and the rate of photosynthesis in phytoplankton. *Ecol Model.* 1988;42:199–215.
38. Rabeh K, Oubohssaine M, Hnini M. TOR in plants: multidimensional regulators of plant growth and signaling pathways. *J Plant Physiol.* 2024;294: 154186.
39. Artins A, Martins MCM, Meyer C, Fernie AR, Caldana C. Sensing and regulation of C and N metabolism—novel features and mechanisms of the TOR and SnRK1 signaling pathways. *Plant J.* 2024. <https://doi.org/10.1111/tj.16684>.
40. Li L, Song Y, Wang K, Dong P, Zhang X, Li F, Li Z, Ren M. TOR-inhibitor insensitive-1 (TRIN1) regulates cotyledons greening in *Arabidopsis*. *Front Plant Sci.* 2015;6:861.
41. Mallen-Ponce MJ, Perez-Perez ME, Crespo JL. Photosynthetic assimilation of CO₂ regulates TOR activity. *Proc Natl Acad Sci U S A.* 2022;119(2): e2115261119.
42. Riegler S, Servi L, Scarpin MR, Godoy Herz MA, Kubaczka MG, Venhuizen P, Meyer C, Brunkard JO, Kalyna M, Barta A, Petrillo E. Light regulates alternative splicing outcomes via the TOR kinase pathway. *Cell Rep.* 2021;36(10): 109676.
43. Canal MV, Mansilla N, Gras DE, Ibarra A, Figueroa CM, Gonzalez DH, Welchen E. Cytochrome c levels affect the TOR pathway to regulate growth and metabolism under energy-deficient conditions. *New Phytol.* 2024;241(5):2039–58.
44. Martin WF, Bryant DA, Beatty JT. A physiological perspective on the origin and evolution of photosynthesis. *FEMS Microbiol Rev.* 2018;42(2):205–31.
45. Ciereszko I. Regulatory roles of sugars in plant growth and development. *Acta Soc Bot Pol.* 2018. <https://doi.org/10.5586/asbp.3583>.
46. Jamsheer MK, Jindal S, Laxmi A. Evolution of TOR–SnRK dynamics in green plants and its integration with phytohormone signaling networks. *J Exp Bot.* 2019;70(8):2239–59.
47. Zhao Y, Wang XQ. In silico analysis of *Vitis vinifera* cabernet sauvignon TOR and its responses to sugar and abscisic acid signaling. *Acta Botanica Brasiliica.* 2022;36:e2020abb0482.
48. Chen EJ, Kaiser CA. LST8 negatively regulates amino acid biosynthesis as a component of the TOR pathway. *J Cell Biol.* 2003;161(2):333–47.
49. Miret JA, Griffiths CA, Paul MJ. Sucrose homeostasis: mechanisms and opportunity in crop yield improvement. *J Plant Physiol.* 2024;294: 154188.
50. Lutt N, Brunkard JO. Amino acid signaling for TOR in eukaryotes: sensors, transducers, and a sustainable agricultural fuTORE. *Biomolecules.* 2022;12(3):387.
51. Roustav V, Bakhtiari S, Roustav PJ, Weckwerth W. Quantitative in vivo phosphoproteomics reveals reversible signaling processes during nitrogen starvation and recovery in the biofuel model organism *Chlamydomonas reinhardtii*. *Biotechnol Biofuels.* 2017;10:280.
52. Gabi Amoroso DS, Thyssen C, Fock HP. Uptake of HCO₃⁻ and CO₂ in cells and chloroplasts from the microalgae *Chlamydomonas reinhardtii* and *Dunaliella tertiolecta*. *Plant Physiol.* 1998;116(1):193–201.
53. Wang Y, Stessman DJ, Spalding MH. The CO₂ concentrating mechanism and photosynthetic carbon assimilation in limiting CO₂: how *Chlamydomonas* works against the gradient. *Plant J.* 2015;82(3):429–48.
54. Krishnan A, Kumaraswamy GK, Vinyard DJ, Gu H, Ananyev G, Posewitz MC, Dismukes GC. Metabolic and photosynthetic consequences of blocking starch biosynthesis in the green alga *Chlamydomonas reinhardtii* *sta6* mutant. *Plant J.* 2015;81(6):947–60.
55. Zabawinski C, Van Den Koornhuise N, D'Hulst C, Schlichting R, Giersch C, Delrue B, Lacroix JM, Preiss J, Ball S. Starchless mutants of *Chlamydomonas reinhardtii* lack the small subunit of a heterotetrameric ADP-glucose pyrophosphorylase. *J Bacteriol.* 2001;183(3):1069–77.
56. Duran RV, Oppliger W, Robitaille AM, Heiserich L, Skendaj R, Gottlieb E, Hall MN. Glutaminolysis activates Rag-mTORC1 signaling. *Mol Cell.* 2012;47(3):349–58.
57. Artins A, Caldana C. The metabolic homeostator: the balance of holding on or letting grow. *Curr Opin Plant Biol.* 2022;66: 102196.
58. Imamura S, Kawase Y, Kobayashi I, Shimojima M, Ohta H, Tanaka K. TOR (target of rapamycin) is a key regulator of triacylglycerol accumulation in microalgae. *Plant Signal Behav.* 2016;11(3): e1149285.
59. Hulatt CJ, Smolina I, Dowie A, Kopp M, Vasanth GK, Hoarau GG, Wijffels RH, Kiron V. Proteomic and transcriptomic patterns during lipid remodeling in *Nannochloropsis gaditana*. *Int J Mol Sci.* 2020;21(18):6946.

Publisher's Note

Springer Nature remains neutral with regard to jurisdictional claims in published maps and institutional affiliations.